

Accepted Manuscript

Title: Optimal Energy Management System based on Stochastic Approach for a Home Microgrid with Integrated Responsive Load Demand and Energy Storage

Author: Mousa Marzband Hamed Alavi Seyedeh Samaneh Ghazimirsaeid Hasan Uppal Terrence Fernando



PII: S2210-6707(16)30444-9
DOI: <http://dx.doi.org/doi:10.1016/j.scs.2016.09.017>
Reference: SCS 519

To appear in:

Received date: 25-4-2016
Revised date: 28-9-2016
Accepted date: 29-9-2016

Please cite this article as: Mousa Marzband, Hamed Alavi, Seyedeh Samaneh Ghazimirsaeid, Hasan Uppal, Terrence Fernando, Optimal Energy Management System based on Stochastic Approach for a Home Microgrid with Integrated Responsive Load Demand and Energy Storage, *Sustainable Cities and Society* (2016), <http://dx.doi.org/10.1016/j.scs.2016.09.017>

This is a PDF file of an unedited manuscript that has been accepted for publication. As a service to our customers we are providing this early version of the manuscript. The manuscript will undergo copyediting, typesetting, and review of the resulting proof before it is published in its final form. Please note that during the production process errors may be discovered which could affect the content, and all legal disclaimers that apply to the journal pertain.

Optimal Energy Management System based on Stochastic Approach for a Home Microgrid with Integrated Responsive Load Demand and Energy Storage

Mousa Marzband^{a,b}, Hamed Alavi^c, Seyedeh Samaneh Ghazimirsaeid^d, Hasan Uppal^a, Terrence Fernando^d

^aSchool of Electrical and Electronic Engineering, Faculty of Engineering and Physical Sciences, Electrical Energy and Power Systems Group, The University of Manchester, Ferranti Building, Manchester, M13 9PL, United kingdom

^bDepartment of Electrical Engineering, Lahijan Branch, Islamic Azad University, Lahijan, Guilan, Iran

^cDepartment of Electrical Engineering, South Tehran Branch, Islamic Azad University, Tehran, Tehran, Iran

^dSchool of the Built Environment, 4th Floor, Maxwell Building Room 712 (THINKlab), University of Salford, Salford, M5 4WT, United kingdom

Abstract

In recent years, increasing interest in developing small-scale fully integrated energy resources in distributed power networks and their production has led to the emergence of smart Microgrids (MG), in particular for distributed renewable energy resources integrated with wind turbine, photovoltaic and energy storage assets. In this paper, a sustainable day-ahead scheduling of the grid-connected home-type Microgrids (H-MG) with the integration of non-dispatchable/dispatchable distributed energy resources and responsive load demand is co-investigated, in particular to study the simultaneously existed uncontrollable and controllable production resources despite the existence of responsive and non-responding loads. An efficient energy management system (EMS) optimization algorithm based on mixed-integer linear programming (MILP) (termed as EMS-MILP) using the GAMS implementation for producing power optimization with minimum hourly power system operational cost and sustainable electricity generation of within a H-MG. The day-ahead scheduling feature of electric power and energy systems shared with renewable resources as a MILP problem characteristic for solving the hourly economic dispatch-constraint unit commitment is also modelled to demonstrate the ability of an EMS-MILP algorithm for a H-MG under realistic technical constraints connected to the upstream grid. Numerical simulations highlights the effectiveness of the proposed algorithmic optimization capabilities for sustainable operations of smart H-MGs connected to a variety of global loads and resources to postulate best power economization. Results demonstrate the effectiveness of the proposed algorithm and show a reduction in the generated power cost by almost 21% in comparison with conventional EMS.

Keywords: Day ahead scheduling, energy management system, microgrid, optimal operation and scheduling, responsive load demand.

Nomenclature

Acronyms

DER	distributed energy resources
ES	energy storage
EMS	energy management systems
UG+, UG-	buying/ selling power from/to H-MG/the upstream grid
H-MG	home microgrid
MILP	mixed integer linear programming
MT	micro-turbine
MCP	market clearing price
NRL	non-responsive load
PV	photovoltaic
ES+, ES-	ES during charging/discharging mode
RLD	responsive load demand
RLD+, RLD-	amount of demand that goes/come from/to other time period to/from t
SOC	state-of-charge

TCP	total consumed power
TGP	total generated Power
WT	wind turbine
Parameters	
P_t^n	the predicted consumed electrical load demand at time t (kW)
P_t^A	available power of A (kW)
$A \in \{WT, PV\}$	
Constants	
ζ_e^B	electrical efficiency of the thermal B th DER in H-MG (%)
π^{ng}	natural fuel price offer (£/kWh)
$\bar{P}^B, \underline{P}^B$	maximum/minimum electrical power generated by B (kW)
$\underline{SOC}, \overline{SOC}$	the lower/ upper limit of SOC (%)
SOC_{INI}	initial SOC (%)
E_{Tot}^{ES}	total capacity of ES (kWh)
$T_{ON}^{MT}, T_{OFF}^{MT}$	turn on/off time (min)
R_l^{MT}, R_u^{MT}	ramp down/up limit (kW)
η	a part of excess/shortage power required by H-MG
ζ^{MT}	MT efficiency (%)

Email address: mousa.marzband@manchester.ac.uk, Tel.

+44(0)1613064654, Fax. +44(0)1613064820.

Corresponding author (Mousa Marzband)

Preprint submitted to Sustainable Cities and Society

September 28, 2016

1	π^B	the supply bids by B (€/kWh)
2	$B \in \{MT, ES-, ES+, RLD+, RLD-, UG+, \& UG-\}$	
3	Δt	time step (h)
4	Decision variables	
5	P_t^B	available power of B (kW)
6	X_t^B	binary variable of B
7	FU_t^{MT}	fuel consumption rate
8	SOC_t	ES SOC (%)
9	$\lambda_t^1 - \lambda_t^8$	MCP at each time t in the following algorithms, respectively:
10		
11	λ_t^1 :	EMS-MILP algorithm
12	λ_t^2 :	EMS unit
13	λ_t^3 :	imperialist competitive algorithm
14	λ_t^4 :	Nikaido's/relaxation algorithm
15	λ_t^5 :	multi-artificial bee colony
16	λ_t^6 :	multi-ant colony optimization
17	λ_t^7 :	multi-gravitational search algorithm
18	λ_t^8 :	mixed integer non-linear programming
19		
20		

21 1. Introduction

22
 23 Future smart buildings will incorporate an increasing non-
 24 dispatchable/dispatchable generation units and energy stor-
 25 age (ES) devices coupled with responsive load demand
 26 (RLD) switching from conventional routines of consumptions
 27 to distributions and regulation counterparts [1]. In specific
 28 RLD loads are of interest because of their interruptible nature,
 29 in contrast with NRLD counterparts of non-interruptible
 30 nature, and being not part of the sensible loads that have the
 31 ability to flexibly respond to the Microgrid's customer finan-
 32 cial encouraging contractual implementations, with respect
 33 to minimizing consumers lead costs while maximizing oper-
 34 ational efficiency by shifting from peak time loading to non-
 35 peak periods. With continuous increase in the growth rate
 36 of home Microgrid (H-MG) and renewable resource pene-
 37 trations for more than a decade unregulated load demand
 38 together with intermittent renewable generation are posing
 39 additional challenges on supply-demand balancing condi-
 40 tions in smart H-MG [2]. H-MG represents a vision for non-
 41 dispatchable/dispatchable distributed generations and con-
 42 sumptions, enhancing the robustness and stability of power
 43 grids and explores new ways of utilizing sustainable energy
 44 resources in terms of new generation of renewable integrated
 45 energy systems [2–5]. Facilitated by recent advances in RLD
 46 and renewable generation, systems are managed adaptively
 47 in response to variations of renewable power supply and load
 48 demand, simultaneously. [6]. These adaptive features com-
 49 bined with the objective of reducing the overall operational
 50 cost of the whole H-MG system, the RLD can play a critical
 51 role as in to offer a fully integrated platform to be collabora-
 52 tively perform features like peak shaving and load shedding
 53 with all considerations of physical, financial, and environ-
 54 mental constrains [7, 8].

55
 56 In H-MG, the issue of supply-demand mismatch with re-
 57 newable energy generation can be made if energy genera-
 58 tion sources are not sufficient enough to supply the load de-
 59 mand and no proper energy management system (EMS) is
 60

employed. A proper EMS is one which makes effective use
 of available distributed energy resources (DERs) optimally,
 while ensuring efficient resources usage and the sustainabil-
 ity of the supply. However, these EMSs have constrictive
 bounds to their operational limits and may also fail to supply
 the load demand if total demand is more than the maximum
 capacity of the generation resources. Under such scenar-
 ios, employing backup systems, such as energy storage (ES),
 and/or applying RLD options helps reduce electricity supply-
 demand unbalance [9–12]. RLD is a mechanism to enable
 customers to participate in the electricity market in order to
 reduce the peak demand by scheduling both power consump-
 tion and operation time for power-shiftable appliances and
 time-shiftable appliances. One of the key objectives of EMS
 with RLD availability is to reduce power consumption in peak
 hours and shifting demand to off-peak hours when cheaper,
 cleaner electricity is available [13–15].

In this paper, an intelligent EMS based on mixed integer
 linear programming (MILP) (EMS-MILP) is designed to eas-
 ily accommodate a wide range of ES and RLD in the grid-
 connected H-MG. as to demonstrate smart grid implementa-
 tion and optimization, presented as an energy management
 system. For all purpose H-MGs, the optimum performance
 of each one of the production resources requires optimized
 management of load demand under different conditions, as
 also considered in this study. Since the model considered for
 the H-MGs is non-linear, the optimization algorithms for find-
 ing the best solution for the efficient and intelligent power
 distribution, in particular for H-MGs connected to the up-
 stream grid, where load demand fluctuations can lead to fre-
 quency variations and reactive power can also be considered
 in this study [16, 17].

The proposed EMS-MILP offers an intelligent mainte-
 nance, regulation and unit scheduling framework for grid-
 integrated H-MG that can be utilized for real-time optimiza-
 tion considering all achieved smart energy generation units
 with improved performance/energy monitoring and reduced
 energy cost. In addition, where DERs have a positive effect
 over electricity market efficiency and reliability of supplying
 power by using revolving reserves, our optimum algorithm
 incorporates the contribution of power for revolving reserves,
 energy storage resources and DERs, all integrated to emulate
 conditions for uncontrollable resources and uninterruptable
 loads, measured in real-time from upstream grid by using
 central controlling unit. The optimum scheduling in this in-
 tegrated structure including generation and DER resources
 combined together also addresses scenarios of maximizing
 performance and minimizing system cost. Moreover, a gen-
 eralized framework model that can adopt for all global con-
 sumers to participate in RLD program is proposed. The main
 contributions of the work are as follows:

- Presenting a stochastic bidding strategy for H-MG par-
 ticipating in local energy market in consideration of un-
 certainties of load demand and available output power
 of wind turbine (WT) and photovoltaic (PV) resources;
- Presenting RLD programming combined with ES is in-
 vestigated under the presence of variable renewable

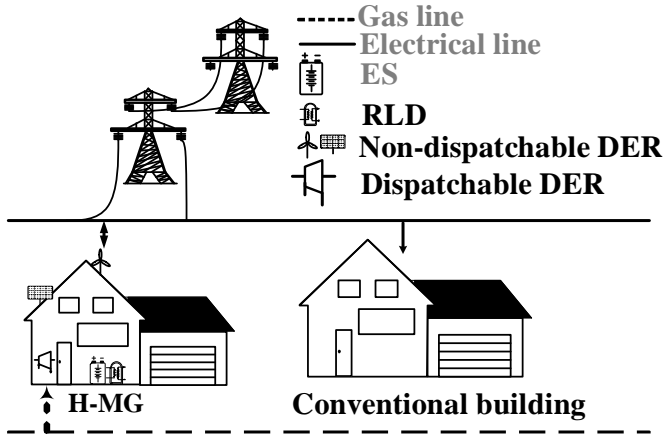


Figure 1: Comparison between a conventional building and H-MG with the integration of non-dispatchable/dispatchable distributed energy resources and responsive load demand.

generated power to demonstrate its ability for DER generation to reduce the market clearing price.

2. Application to test grid

The schematic diagram of a grid-connected H-MG which is main focus of this paper is illustrated in Figure 1. In this configuration, dispatchable/non-dispatchable DERs and ES devices and associated RLD are configured in H-MG. To begin, EMS-MILP receives data including the generated power by non-dispatchable DERs and the non-responsive load (NRL) demand, the general properties of each DERs (such as maximum/minimum power generated by them, the turning on and turning off time of non-dispatchable DER as presented in Table 1), ES SOC. Then, all the optimal power set-points of each DERs and RLD will be dispatched to them at each time interval based on the proposed EMS. Simulation evaluations are performed for a grid-connected H-MG including wind turbine (WT), photovoltaic (PV), microturbine (MT), and energy storage (ES). The real life experimental data carried out from [15] are also used to simulate WT, PV and NRL demand. The WT, PV, and NRL demand profiles are shown in Figure 2.

For investigating the proposed algorithm performance correctness in encountering different incidents, three scenarios have been implemented over the grid-connected H-MG under study: (the SOC initial value (i.e. SOC_{INI}) in all the scenarios has been set equal to 50%).

Scenario #1: normal operation.

Scenario #2: sudden increase in load demand.

Scenario #3: emergency shut-down at non-dispatchable resources.

3. Problem formulation

3.1. Objective function

Our first attempt considers defining the objective function as a problem structure that includes profit negative values

Table 1: Configuration parameters for each non-dispatchable/dispatchable DER and ES resources

Parameter	symbol	Value
ES system		
Voltage (V)	V_t^{ES}	24
Nominal Ah capacity at +25°C	N_t^{ES}	84
Fully Charged voltage (V)	\bar{V}^{ES}	26
Cut-Off discharge voltage (V)	\underline{V}^{ES}	21
Maximum continuous charge current (A)	\bar{I}^{ES+}	34
Maximum continuous discharge current (A)	\bar{I}^{ES-}	160
Maximum battery power during charging Mode (kW)	\bar{P}^{ES+}	0.816
Maximum battery power during discharging Mode (kW)	\bar{P}^{ES-}	3.84
Maximum delivered power by converter (kW)	\bar{P}^{ES}	4
Initial SOC (%)	SOC_{INI}	50
Maximum SOC (%)	SOC	80
Minimum SOC (%)	SOC	20
Initial stored energy in battery (kWh)	E_{INI}^{ES}	1
Maximum stored energy in ES (kWh)	\bar{E}^{ES}	1.6
Minimum stored energy in ES (kWh)	\underline{E}^{ES}	0.403
Total capacity of ES (kWh)	E_{tot}^{ES}	2
Charge efficiency factor (%)	η_c	96
PV system		
Maximum instantaneous power for PV (kW)	\bar{P}^{PV}	6
Minimum instantaneous power for PV (kW)	\underline{P}^{PV}	0
WT system		
Maximum instantaneous power for WT (kW)	\bar{P}^{WT}	8
Minimum instantaneous power for WT (kW)	\underline{P}^{WT}	0.45
MT system		
Maximum instantaneous power (kW)	\bar{P}^{MT}	12
Minimum instantaneous power (kW)	\underline{P}^{MT}	3.6
Turn on time (min)	T_{ON}^{MT}	6
Turn off time (min)	T_{OFF}^{MT}	6
Ramp down limit (kW)	R_{\downarrow}^{MT}	6
Ramp up limit (kW)	R_{\uparrow}^{MT}	6

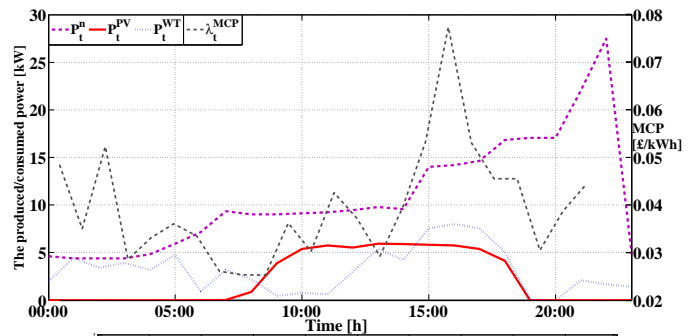


Figure 2: NRL load demand profile comparison for power produced by PV, WT resources and the predicted MCP profile based on the hourly experimental data adapted from [15, 18].

1 that requires minimization via EMS optimization. Although,
 2 the above function can be fully extended to integrate other
 3 variables, constraints and balancing conditions to include
 4 other technical and environmental aspects for a given H-MG.
 5 values that requires minimization via EMS optimization. Al-
 6 though, the above function can be fully extended to integrate
 7 other variables, constraints and balancing conditions to in-
 8 clude other technical and environmental aspects for a given
 9 H-MG. Profit negative is equal to the overall cost of gener-
 10 ating electricity by the H-MG without the H-MG incomes
 11 stream. The defined objective function for a grid-connected
 12 H-MG thereby can be expressed as follows.

$$13 \quad Z = \min \left[\sum_{t=1}^{24} \left(\begin{aligned} & (FU_t^{MT} \times \pi_t^{ng} + p_t^{ES+} \times \pi_t^{ES+} \\ & + p_t^{RLD+} \times \pi_t^{RLD+} + p_t^{UG-} \times \pi_t^{UG-}) \\ & - (p_t^{WT} \times \pi_t^{WT} + p_t^{PV} \times \pi_t^{PV} \\ & + p_t^{ES-} \times \pi_t^{ES-} + p_t^{MT} \times \pi_t^{MT} \\ & + p_t^{UG+} \times \pi_t^{UG+} + p_t^{RLD-} \times \pi_t^{RLD-}) \end{aligned} \right) \times \Delta t \right] \quad (1)$$

14 Subject to:

15 • **power balance**

$$16 \quad p_t^{WT} + p_t^{PV} + p_t^{ES-} + p_t^{MT} + p_t^{UG-} \times (1 - \chi_t^{UG}) = p_t^n + p_t^{ES+} \\ 17 \quad + p_t^{RLD+} \times (1 - \chi_t^{RLD}) - p_t^{RLD-} \times \chi_t^{RLD} + p_t^{UG+} \times \chi_t^{UG} \quad (2)$$

18 • **Supply/consumer bids**

$$19 \quad \underline{\pi}^B \leq \pi_t^B \leq \bar{\pi}^B \quad (3)$$

20 where $\underline{\pi}^B$ and $\bar{\pi}^B$ are respectively the minimum and
 21 maximum offer of the electrical price in the B^{th} DER.
 22 $\bar{\pi}^B$ can be considered the equivalent of the value of
 23 predicting electrical MCP of the day before imple-
 24 menting uncertainty. $\underline{\pi}^B$ can be considered zero for
 25 non-dispatchable DER generation resources and for re-
 26 sources which consume fuel can be estimated by calcu-
 27 lating electrical marginal cost (MC_e) value of the desired
 28 resource. MC_e for fuel consuming resource is calculated
 29 from the following relation:

$$30 \quad MC_t^B = \frac{P_t^B}{\zeta_e^B} \times \pi^{ng} \quad (4)$$

31 • **non-dispatchable resources (WT and PV in this study)** [15, 19, 20]

$$32 \quad \underline{p}^{PV} \leq p_t^{PV} \leq \bar{p}^{PV} \quad (5)$$

$$33 \quad \underline{p}^{WT} \leq p_t^{WT} \leq \bar{p}^{WT} \quad (6)$$

34 • **dispatchable resources (MT in this study)**

35 – turn on/turn off limit

$$36 \quad \chi_t^{MT} - \chi_{t-1}^{MT} - e_t^{MT} + a_t^{MT} = 0 \quad (7)$$

$$37 \quad a_t^{MT} + \sum_{k=t}^{\delta_{t1}} e_k^{MT} \leq 1, \delta_{t1} = \min\{t + T_{ON}^{MT}, T\} \quad (8)$$

$$38 \quad e_t^{MT} + \sum_{k=t}^{\delta_{t2}} a_k^{MT} \leq 1, \delta_{t2} = \min\{t + T_{OFF}^{MT}, T\} \quad (9)$$

39 χ_t^{MT} is a binary variable which shows the off or on
 40 condition of unit MT at time t , when the unit is

41 on. It allocates the one value to itself and other-
 42 wise its value is zero. a_t^{MT} and e_t^{MT} are also binary
 43 variables which their condition regarding the unit
 44 exploitation conditions change. If $\chi_{t-1}^{MT}=1$ ($a_t^{MT}=1$
 45 will become one and when $e_t^{MT}=1$ if $\chi_{t-1}^{MT}=0$ and
 46 χ_t^{MT} when $a_t^{MT}=e_t^{MT}=0$ if $\chi_t^{MT}=1$ and $\chi_{t-1}^{MT}=0$)

47 – ramp up and down limit [21, 22]

$$48 \quad R_u^{MT} \leq (p_t^{MT} - p_{t-1}^{MT}) \leq R_d^{MT} \quad (10)$$

49 – MT generation limit

$$50 \quad \chi_t^{MT} \cdot \underline{p}^{MT} \leq p_t^{MT} \leq \chi_t^{MT} \cdot \bar{p}^{MT}, \chi_t^{MT} \in \{0, 1\} \quad (11)$$

51 – fuel consumption rate

$$52 \quad FU_t^{MT} = p_t^{MT} / \zeta^{MT} \quad (12)$$

53 • **ES constraints** [14, 19]

54 – maximum discharge limit

$$55 \quad p_t^{ES-} \leq \bar{p}^{ES-} \times \chi_t^{ES}, \chi_t^{ES} \in \{0, 1\}, p_t^{ES-} \geq 0 \quad (13)$$

56 – maximum charge limit

$$57 \quad p_t^{ES+} \leq \bar{p}^{ES+} \times (1 - \chi_t^{ES}), p_t^{ES+} \geq 0 \quad (14)$$

58 – maximum discharge limit considering the stored
 59 energy

$$60 \quad (p_t^{ES-} \times \Delta t) \leq E_{t-1}^{ES} \quad (15)$$

61 – Maximum charge limit considering the stored en-
 62 ergy

$$63 \quad ((p_t^{ES+} \times \Delta t) + E_{t-1}^{ES}) \leq \bar{E}^{ES} \quad (16)$$

64 – energy balance

$$65 \quad E_t^{ES} = E_{t-1}^{ES} + (p_{t-1}^{ES+} - p_{t-1}^{ES-}) \times \Delta t \quad (17)$$

66 – ES SOC

$$67 \quad SOC_t = \frac{E_t^{ES}}{E_{Tot}^{ES}} \quad (18)$$

68 – energy stored limit

$$69 \quad \underline{E}^{ES} \leq E_t^{ES} \leq \bar{E}^{ES} \quad (19)$$

70 • **RLD constraints**

71 On the other hand, the amount of power allocated for
 72 the RLD can be specified by EMS-MILP incorporates the
 73 technical and economic constraints. After determining
 74 the optimum set-point powers of each DERs and the
 75 value of surplus and shortage powers, this information
 76 will be spontaneously sent to the RLD unit. For the
 77 first time, our novel EMS-MILP implementation incor-
 78 porates all constraints for RLD/DER where household
 79 consumed loads for a H-MG are classified as both in-
 80 interruptible loads (i.e. RLD) and no interruptible loads
 81 (i.e. NRLD), respectively. For generated power in H-MG,
 82 the generation resources are more than the consumption
 83 amount by the consumers (i.e. at the beginning of the
 84 day) thereby excess generation is created, and the pro-
 85 posed EMS algorithm during operational times decides
 86 to supply RLD+ loads:

$$87 \quad p_t^{TCP} = p_t^n + p_t^{ES+} + p_t^{RLD+} + p_t^{UG+} \quad (20)$$

88 Also, when power shortage exists in the H-MG (i.e. at
 89 the end of the day) and the amount of generation re-
 90 sources is less than the amount of consumed power,

the proposed EMS transfers interruptible loads from this time interval to other time intervals for helping system stability:

$$P_t^{TGP} = P_t^{WT} + P_t^{PV} + P_t^{MT} + P_t^{ES-} + P_t^{RLD-} + P_t^{UG-} \quad (21)$$

$$P_t^{RLD-} \leq (P_t^{TCP} - P_t^{TGP}) \times X_t^{RLD} \quad (22)$$

$$\sum_{t=1}^{24} (P_t^{RLD+} \times (1 - X_t^{RLD})) = \sum_{t=1}^{24} (P_t^{RLD-} \times X_t^{RLD}) \quad (23)$$

• **upstream grid constraints**

$$\bar{P}^{UG} \leq \eta \times (P_t^{WT} + P_t^{PV} + P_t^{MT} + P_t^{ES-}) \quad (24)$$

$$P_t^{UG-} \leq \bar{P}^{UG} \times (1 - X_t^{UG}) \quad (25)$$

$$P_t^{UG+} \leq \bar{P}^{UG} \times X_t^{UG} \quad (26)$$

The above implementation signifies the functional ability of GAMS/EMS-MILP objective function to study the increase of energy generation shared under renewable resources, where a co-optimization of maximizing profit and/or minimizing cost considered with all technical constraints of load supply for all resources in the H-MG. In addition, where simultaneous use of renewable energy generation resources and energy storing/battery resources along with responsive loads creates complexities for multiscale H-MG energy management, the proposed algorithm also successfully adapts to the above structure. Determining that what amount of load demand can be shifted/supplied to/from a time interval to another is one of key roles of the RLD unit.

3.2. Mixed-Integer Linear Programming Optimization

A mixed-integer linear program optimization is applied to the above objective function as; problem with:

- For linear objective function of $f^T x$, where f is a column vector of constants, and x is the column vector of unknowns.
- All bounds are considered as linear constraints, and no nonlinear constraints have been defined.
- The restrictions on some components of x to have integer values is also applied.

In mathematical terms, given vectors f , lb , and ub , matrices A and Aeq , corresponding vectors b and beq , and a set of indices $intcon$ are defined to compute a vector x to solve:

$$\min_x f^T x \text{ subject to } = \begin{cases} x \text{ is integers} \\ A \cdot x \leq b \\ Aeq \cdot x = beq \\ lb \leq x \leq ub \end{cases} \quad (27)$$

where integer variables must take an integer value (0, 1, 2, ...). A unique integer variables is a binary variables that can only take the value 0 or 1, where a maximum of 1 and implicitly a minimum of 0 on each variable are constrictive bounds at all times. If all variables are integer then it is a pure integer model, else it is a mixed-integer model, sometimes denoted as MIP (Mixed Integer Programming).

4. The proposed EMS-MILP

The EMS-MILP proposed in this paper is depicted in Figure 3. This algorithm is encompassed from two part namely EMS-MILP and conventional EMS. EMS-MILP will be executed if switches of S1 and S2 have the status of ON and OFF, respectively. Conventional EMS is based on method without optimization algorithm. It comprises different units, i.e. economic dispatch (ED) unit, RLD unit, Taguchi's orthogonal array testing (TOAT) unit and market clearing price (MCP) unit. The relationship between these four units is shown in this figure. As observed, information such as the technical constraints of the devices involved in the H-MG, prediction of the NRL demand and the non-dispatchable generation resources and offers of each existing resources in the H-MG are sent to the TOAT unit. TOAT is used to represent the probability distribution of the intermittent supply from non-dispatchable DERs, NRL and MCP profiles as addressed in literature [12]. After applying uncertainty over the inputs, the total consumed power (TCP) and the total generated power (TGP) can be determined in ED unit by solving minimization problem based on an objective function subject to the constraints described in section 3. After selecting the H-MG operation mode (islanded or grid-connected) and by introducing a binary variable (i.e. X_t^{UG}), ED unit is computed and executed completely independent, irrespective of the optimum power values of the existing dispatchable and non-dispatchable DERs and NRL demands. Since the H-MG under consideration is operated in an islanded mode, there will be no power trade-off between/ with the upstream grid. On the other hand, the grid connected H-MG can also make it possible to exchange information on power generation and consumption between H-MG and upstream grid. Noting the objective function and offers of the existing DERs in the H-MG, the excess power generation can be supplied to the upstream grid. RLD is also considered to be an alternative energy resource to keep this power in the H-MG instead of release it to the upstream grid. It can often help reduce the amount of power the corporation has to generate from expensive fossil fuels by dispatchable DER. EMS-MILP specifies based on the minimization of objective function (e.g. profit negative or operation cost), decides whether power exchange with the outside is beneficial for the MG owner or not. On the other hand, the amount of power allocated for the RLD can be specified by EMS-MILP incorporates the technical and economic constraints. After determining the optimum set-point powers of each DERs and the value of surplus and shortage powers, this information will be spontaneously sent to the RLD unit. For the first time, our novel EMS-MILP implementation incorporates all constraints for DR/DER where household consumed loads for a H-MG are classified as both interruptible loads (i.e. RLD) and noninterruptible loads (i.e. NRLD), respectively. For generated power in H-MG, the generation resources are more than the consumption amount by the consumers (i.e. at the beginning of the day) thereby excess generation is created, and the proposed EMS algorithm during operational times decides to supply RLD+ loads.

Also, when power shortage exists in the H-MG (i.e. at the end of the day) and the amount of generation resources is less than the amount of consumed power, the proposed EMS transfers interruptible loads from this time interval to other time intervals for helping system stability.

Determining that what amount of load demand can be shifted/supplied to/from a time interval to another is one of key roles of the RLD unit. The exchange of information between RLD and ED units performs the optimum scheduling via minimizing production cost and using both controllable and non-dispatchable resources, the variables transferred between these units are illustrated in Figure 3. EMS unit receives power production information from different production and energy storage units during each time period followed by the performance optimization for MGs. ED unit determines the MG production units optimum level with the least exploitation cost considering technical and economic constraints. RLD unit performs equilibrium between the supply and demand for active load-defined reduction in MG production units to supply load demand, when load demand shift for different times cannot be provided directly. Controllable loads (i.e. RLD) also requires power supply when excess production exists in the system, which is also facilitated by RLD. Overall integration successfully delivers optimum power balance conditions for a diverse nature of resources connected to the microgrid. After obtaining all power set-points and supply/consumer bids by using ED unit, all information must be dispatched to MCP unit. This unit makes the determination of MCP value possible that is the participation optimum powers in the market which are obtained through the ED unit. The process of this unit is implemented as shown in Figure 4. In this flowchart, N_g and N_c are the equal to the number of generating and consuming agents in the electricity market, respectively. The proposed EMS-MILP algorithm is illustrated by a Pseudo-code in Algorithm 1.

5. Results and discussion

The proposed structure is validated over a case study which contains a grid-connected H-MG with different type of generation and consumer units. For this study, an H-MG has been configured by one PV (6 kW), one WT (8 kW), one MT (12 kW), one ES (2 kWh), and responsive/non-responsive load demand.

Figure 5 shows state-of-charge (SOC) in the charge and discharge modes for the proposed algorithm. As demonstrated in this figure, during the time interval 00:00-06:00 the SOC value has not changed that much, at the beginning of interval because ES has acted in the charge mode the value of SOC has acted in the charge mode the value of SOC has reached to \overline{SOC} , and then by discharging and charging ES in the next hours, the SOC value at the end of this interval has approximately approached its initial value. As it is observed during the time interval 06:00-12:00, the increasing load demand and reduction in renewable generation (compared to the previous time intervals), the EMS decided to partially use ES to supply the shortage in power. The value of SOC in this

Input prediction data

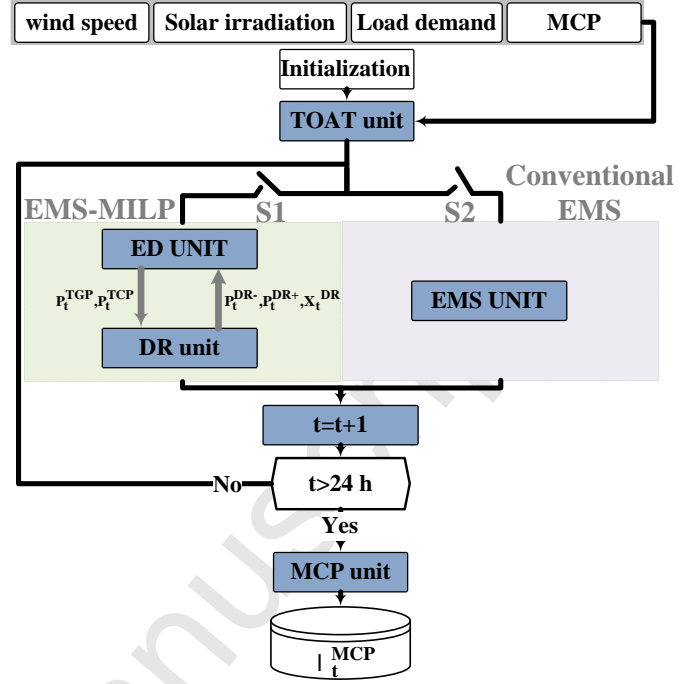


Figure 3: Proposed EMS-MILP algorithm implementation consisting of load response RLD and economic distribution ED units.

Algorithm 1 EMS-MILP ALGORITHM

Require: Initialization \triangleright Hourly prediction data of MG, \overline{SOC} , \underline{SOC} , \overline{P}_t^{MT} and \underline{P}_t^{MT} ,
while $t \leq 24$ do
1. **TOAT unit**
Generate power scenarios randomly for WT, PV and NRL with the probability of occurrence.
2. $P_t^{TGP} = P_t^{WT} + P_t^{PV}$ and $P_t^{TCP} = P_t^n$;
3. if $P_t^{TGP} = P_t^{TCP}$ then
The generated power will be spent supplying the main load by WT and PV.
4. else if $P_t^{TGP} \geq P_t^{TCP}$ then
 $P_t^{EGP} = P_t^{TGP} - P_t^{TCP}$ \triangleright EGP: Excess generated power
5. if $SOC_t \leq \overline{SOC}$ then
6. if $P_t^{EGP} \leq \overline{P}_t^{ES+}$ then
7. Isolated mode: Charging ES (P_t^{ES+}), supplying RLD ($P_t^{RLD+} = P_t^{EGP} - P_t^{ES+}$)
8. Grid connected: Charging ES (P_t^{ES+}), supplying RLD (P_t^{RLD+}), Selling to upstream grid ($P_t^{UG+} = P_t^{EGP} - P_t^{ES+} - P_t^{RLD+}$)
9. else
10. Isolated mode: Charging ES ($P_t^{ES+} = \overline{P}_t^{ES+}$), supplying RLD ($P_t^{RLD+} = P_t^{EGP} - P_t^{ES+}$)
11. Grid connected: Charging ES ($\overline{P}_t^{ES+} = P_t^{ES+}$), supplying RLD (P_t^{RLD+}), Selling to upstream grid ($P_t^{UG+} = P_t^{EGP} - P_t^{ES+} - P_t^{RLD+}$)
12. else if
13. else \triangleright Fully charged mode
14. Isolated mode: supplying RLD ($P_t^{RLD+} = P_t^{EGP}$)
15. Grid connected: supplying RLD (P_t^{RLD+}), Selling to upstream grid ($P_t^{UG+} = P_t^{EGP} - P_t^{RLD+}$)
16. end if
17. else if $P_t^{TGP} \leq P_t^{TCP}$ then
 $P_t^{TCP} - P_t^{TGP} = P_t^{SGP}$ \triangleright SGP: Shortage generated power
18. if $P_t^{SGP} \leq \underline{P}_t^{MT}$ then
19. Turning on MT with $P_t^{MT} = \underline{P}_t^{MT}$ and $P_t^{ES+} = P_t^{MT} - P_t^{SGP}$
20. else if $P_t^{SGP} \leq \overline{P}_t^{MT}$ then
21. $P_t^{MT} = P_t^{SGP}$
22. else if $SOC_t \leq \underline{SOC}$ then \triangleright Fully discharged mode
23. $P_t^{MT} = \overline{P}_t^{MT}$ and $P_t^{RLD-} = P_t^{SGP} - P_t^{MT}$.
24. else if $\overline{P}_t^{ES-} + \overline{P}_t^{MT} \geq P_t^{SGP}$ then
25. Supplying generation shortage by using MT and ES.
26. else
27. $P_t^{ES-} = \overline{P}_t^{ES-}$, $P_t^{MT} = \overline{P}_t^{MT}$ and $P_t^{RLD-} = P_t^{SGP} - (P_t^{MT} + P_t^{ES-})$
28. end if
29. end if
end while
return Return determine the optimum capacity and profit of the all players.

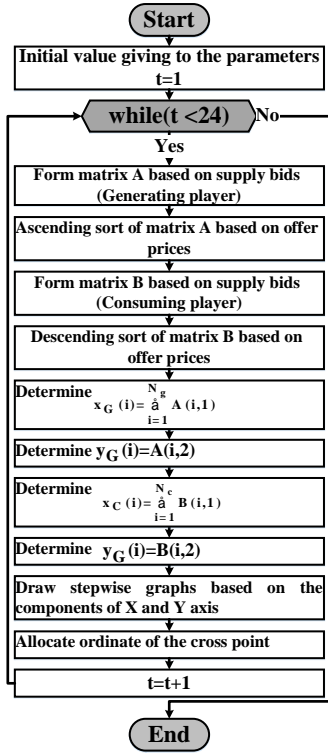


Figure 4: Proposed MCP unit algorithm

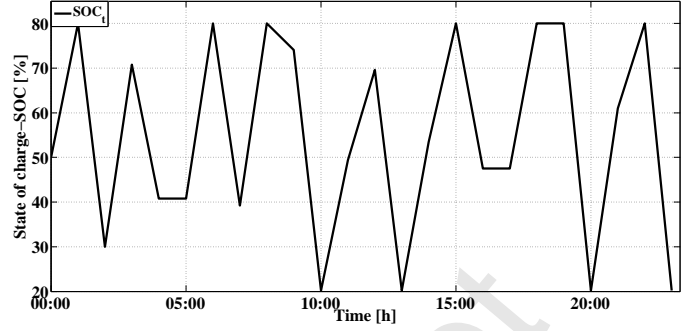


Figure 5: SOC condition during the system 24 hours performance

total load demand. As a result, the ES is commanded by the EMS to cover the rest of the load demand. This way, battery SOC reaches to $\overline{\text{SOC}}$ at the end of the day. It is mentionable in this time interval, the value of SOC in 50% of the times has reached to $\overline{\text{SOC}}$ which shows the adequate performance of the proposed algorithm in managing the energy stored in ES. Generally during the total 24 hours time interval, as for the highness of ES price bid in the discharge mode relation to MT, about 42% of the times ES has been used for supplying the consumed load (discharge mode), about 12% of the times idle (nor in the charging mode nor in the discharging mode) and about 46% of the times ES has been in the charging mode; so more charge has remained in it for essential times. As illustrated in this figure, more than 50% of the times during the system 24 hours performance, the value of SOC has been more than 50% which this fact shows the good support of load demand by ES in the proposed algorithm. It must be noted initialization conditions are based on a balanced SOC consideration be equal to $\sim 50\%$, under the maximum and minimum SOC bounds of 80% and 20% because $E_{\text{Tot}}^{\text{ES}}$ and E_1^{ES} are respectively considered equal to 2 and 1 kWh, thereby initial $\text{SOC}_t = \frac{E_1^{\text{ES}}}{E_{\text{Tot}}^{\text{ES}}}$ equals to $\sim 50\%$. As SOC_t is the energy storage state-of-charge and $E_{\text{Tot}}^{\text{ES}}$ is the total energy stored in ES (battery system our case), the presented model has no bearing on ES overall capacity, and/or SOC initialization conditions on the final simulated results. In Figure 6, the bar-graph related to power generated by generation resources has been shown. As it is obvious during the interval 00:00 to 06:00, MT has been in service during all this time interval always with its minimum power (P^{MT}) and EMS in addition to supplying the NRL consumed load demand and charging ES, has spent excess power supplying RLD. As it is observable from the figure, wind turbine is always in service in this time interval and photovoltaic because of lack of sunshine has been out of service. During the time interval 06:00-12:00, MT is always in service and during the first half of this interval (06:00-09:00), because the NRL load demand has increased relative to the previous interval and renewable resources operate with their low production capacity, EMS for supplying the NRL required power has to use more MT production capacity, but in the end half of this interval because PV resource power has increased, MT operates in service with its minimum power. Generally MT has always been in service

time interval fluctuates. Such that at the beginning of this interval the SOC value has its maximum value (i.e. $\overline{\text{SOC}}$), then because EMS decides to use ES, the value of SOC at 10:00 o'clock has reached to $\underline{\text{SOC}}$. Generally in this interval, ES in 50% of the times is in the charging state and in 50% of the times operate in the discharging mode. At the beginning of this interval 12:00-18:00, because of not using MT for supplying load demand, EMS has used ES for helping to supply demand and as a result is in discharging mode and SOC value at 13:00 has reached to $\underline{\text{SOC}}$. Because of the suitable climate conditions for producing renewable resources the EMS has decided to use these resources with high capacity, not only satisfying NRL and ES charging consumption but also causing the generation of excess power, so EMS has spent the excess generated power supplying RLD. At the beginning of hour 15:00, the battery SOC reaches to its maximum limit. As a result, MT shut down is requested by the EMS while renewable resources are generating at the maximum available rates. During hour 15:00 and 16:00, scenario #2 is observed where the ES is utilized to supply load demand while MT is shut down. The battery SOC at the end of this interval will be reduced which is reasonable.

In the time interval 18:00-24:00, because of the occurrence of scenario #3, the proposed EMS at 19:00 has decided to use ES, so out of necessity the battery has discharged such that the value of SOC at 20:00 o'clock has reached to $\underline{\text{SOC}}$. Scenario #3 occurred during 18:00-24:00 time interval when load demand is at peak. In this case, MT is producing at the rated power (P^{MT}). However, it is not enough to satisfy the

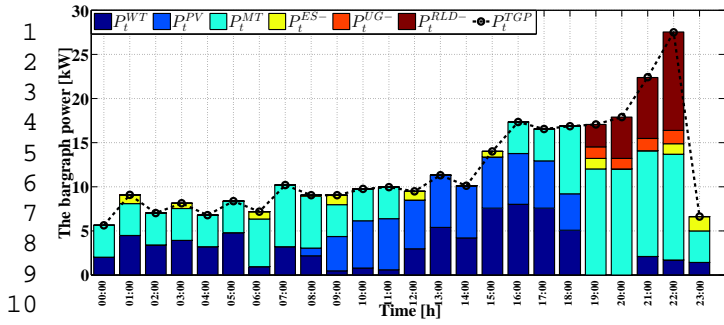


Figure 6: Barograph related to the power produced by generation resources

in this time interval and EMS in addition to supplying the NRL required power and charging ES, has spent excess generated power supplying RLD power. During the time interval 12:00-18:00 scenario #2 has occurred. As for the suitable climatic conditions for generating renewable generation resources, these resources have been put to service with their high capacity and because of the lower price bid of renewable resources relative to MT, the proposed EMS has made a correct decision for turning off MT about 67% of the times which causes the system total cost reduction.

As for the occurrence of scenario #2 in this time interval, it is observable that the proposed algorithm has supplied the power required by NRL and power required by ES for charging and has spent the excess power created supplying RLD power which shows the good algorithm performance for optimum use of production resources and satisfying the consumers demand with the objective of minimizing the total cost of H-MG. Also ES in this interval has operated in the discharging mode about 34% of the times. During the interval 18:00-24:00, scenario #3 has occurred. MT despite higher price bid relative to renewable resources has been in service 67% of the time with its maximum capacity (\bar{P}^{MT}), to supply load. Because of the increase of load demand in this time interval, EMS cannot satisfy the total consumption demand. As a result the EMS has attempted to buy power from the upstream grid (P_t^{UG-}) and shift consumption load (P_t^{RLD-}) to other hours. Generally during the total 24% time interval, about 83% of the times the designed EMS has attempted to use MT. Also, regarding renewable generation resources, WT has been in service about 92% of the times and PV has been in service about 46% of the time. So the proposed EMS has tried all its effort for supplying the consumed load by using these resources, because producing these resources has no cost for the H-MG, as a result supplying the consumed load with these resources will bring more profit for the H-MG.

In Figure 7, the bar-graph of the power consumed by consuming resources has been shown in each time interval. In the time interval 00:00-06:00 the value of NRL load relative to other time intervals is much less and the proposed EMS in addition to supplying the NRL total demand and charging ES, has supplied the RLD power. About 11% of NRL total load demand and about 65% of total RLD power participation share is located in this time interval. During the time

interval 06:00-12:00 the amount of NRL load demand has reduced relative to the previous time interval and the proposed EMS has spent a small amount of the excess power supplying RLD power. In addition to supplying total NRL demand, at 07:00, 10:00 and 11:00 o'clock, the EMS has supplied the ES charging consumption. About 20% of total NRL demand is in the time interval 12:00-18:00. In this time interval, despite the occurrence of scenario #2 and the increase of consumption demand relative to previous intervals, and although only about 9% of total generated power in this time interval is related to MT (about 67% of the time MT is out of service), but because of suitable climate conditions for producing renewable resources with high capacity, excess production has been created. In addition to supplying total NRL demand and charging ES, the EMS has spent excess power supplying RLD. This shows the adequate performance of proposed algorithm in the occurrence of scenario #2. During the time interval 18:00-24:00, scenario #3 has occurred, as has the system load demand peak has occurred and about 40% of the total NRL power demand. But because production resources cannot supply the total load demand in this interval, EMS is forced to shift consumed load (P_t^{RLD-}) to the other hours of the day and to buy power from the upstream grid (P_t^{UG-}). At the end of this time interval, because of the reduction of consumption demand, excess generated power has been allocated to supplying RLD power.

It is notable that about 25kW of created excess consumption has been shifted to other hours and about 5kW has been estimated through buying power from the upstream grid (P_t^{UG-}). Also, as can be observed, the H-MG under study has not allocated excess power for selling to the upstream grid, that is it has spent all the excess generated power supplying RLD and charging ES. Figure 8 is related to RLD+ and RLD- curves and NRL load demand during the system 24 hours performance. From this figure it is observable that in the final hours of the day the amount of load demand is much more than other times; as a result the EMS has attempted to shift consumed load to other hours of the day, so that about 17% of the times during the total system 24 hours interval the EMS has attempted to shift consumed load to other hours, namely 19:00, 20:00, 21:00 and 22:00 in which the system load peak has occurred. As shown in this figure, proposed EMS at the early hours of the day and during sunset has allocated a power for RLD. Generally during the total 24 hours interval, EMS successfully supplies 50% of the times the responsive loads, being the primary allocated power fraction for supplying responsive load for the initial time interval 00:00-06:00. The excess power is generated when RLD+ occurs at the beginning of the day since NRLD load demand is low, and this power is already spent supplying RLD+. In comparison, RLD- occurs when excess consumption is proposed and the system cannot supply load consumption from other production resources. In specific, RLD- ensues at the end of the day relative to other times since for that period the load demand increases for the proposed EMS algorithm that shifts the excess consumption to other times for maintaining overall system stability under balancing conditions. After per-

1 forming scheduling using the RLD constraints of Eq. 23, the
 2 sum of shifted power from all intervals to other time inter-
 3 vals (RLD-) equals to the sum of the value of RLD+ supplied
 4 to load. EMS supplies 50% of times the responsive loads,
 5 where allocated power for supplying responsive load is re-
 6 lated to the time interval 00:00-06:00. The excess power is
 7 generated under RLD+ only at the beginning of the day, since
 8 NRLD load demand is low, and this power is spent supplying
 9 RLD+. Although, RLD- occurs when excess consumption is
 10 proposed and system cannot supply load consumption from
 11 other production resources, generally at the end of the day
 12 because load demand increases for the proposed algorithm
 13 shifts for excess consumption to other times for maintaining
 14 system stability.

15
 16
 17
 18 The values of MCP obtained by EMS-MILP algo-
 19 rithm (λ_t^1), without optimization algorithm (EMS unit)
 20 (λ_t^2), imperialist competitive algorithm (ICA) (λ_t^3) [12],
 21 Nikaido's/relaxation algorithm (NIRA) (λ_t^4) [22],
 22 multi-artificial bee colony (MABC) (λ_t^5) [3], multi-ant
 23 colony optimization (MACO) (λ_t^6) [19], multi-gravitational
 24 search algorithm (MGSA) (λ_t^7) [4], mixed integer non-linear
 25 programming (MINLP) (λ_t^8) [14] is shown in Figure 9. As
 26 depicted in this figure, demand side strategy applied in
 27 EMS-MILP algorithm has had a significant effect in reducing
 28 the MCP value in almost all of the time intervals. MCP
 29 values obtained from EMS unit are higher than those from
 30 EMS-MILP algorithm in all of time intervals when H-MGs
 31 operate by the proposed algorithm. In particular, the
 32 difference between λ_t^1 , λ_t^2 and λ_t^3 has respectively reached
 33 79% and 92% of time intervals; considering that it has
 34 undergone even more intense reduction under λ_t^4 up to 33%
 35 of time intervals than any other algorithms. It is worthful
 36 to mention here that the maximum and minimum values
 37 of MCPs have had significant reduction in all the possible
 38 scenarios as seen in Figure 9. This is while the maximum
 39 value of λ_t^1 is reached by 4% to 28% in comparison with
 40 MCP under different algorithm. In addition, the minimum
 41 value of $\lambda_{t,e}^1$ has shown more reduction (between 17% and
 42 96%) relative to MCP in all the implemented algorithm.
 43 The proposed demand side management among H-MGs un-
 44 doubtedly had considerable effect in lowering the maximum
 45 values of MCP especially with respect to case that H-MGs
 46 are allowed to work more independently. This is while the
 47 maximum value of MCP is negligibly increased under λ_t^8 ,
 48 but its minimum value is significantly reduced under λ_t^1 .
 49 By comparing the values of λ_t^1 and λ_t^2 shown in Figure 9,
 50 when MCP has its maximum value under all time interval,
 51 EMS-MILP algorithm has tried to motivate the customers
 52 shift their demand to off-peak period when MCP is lower
 53 and when it is more convenient for the H-MG to produce
 54 electricity. Regarding the minimum value of λ_t^1 , it is relevant
 55 to mention that it has occurred at the early hours of the day
 56 in all the possible condition in which a significant reduction
 57 in the value of λ_t^1 is observed at the end of the day.

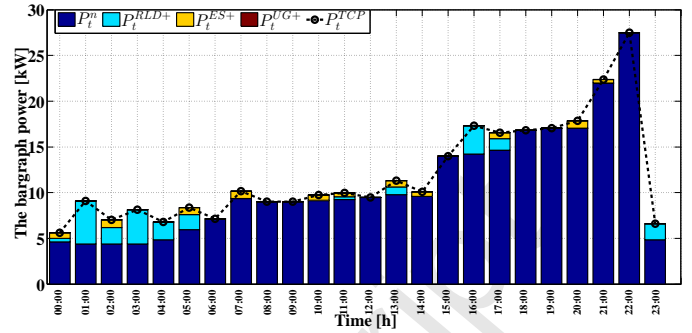


Figure 7: Bargraph related to the consumed power by consumers

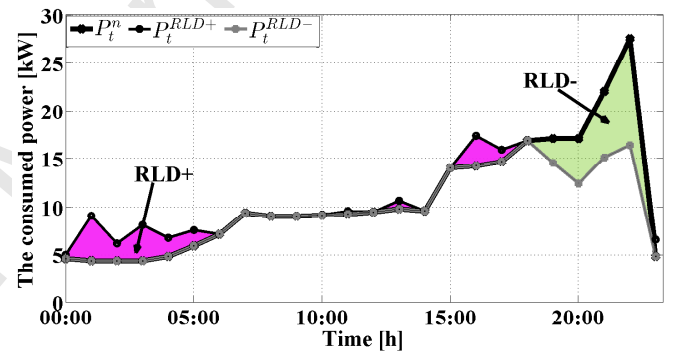


Figure 8: RLD+ and RLD- load demand profile comparison for EMS system over 24 hours performance benchmark.

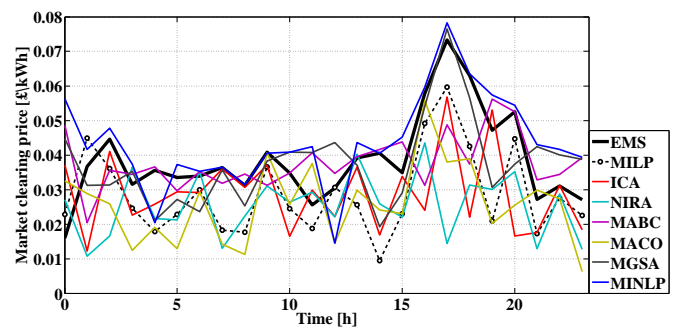


Figure 9: Electrical MCPs in the different optimization algorithms

6. Conclusions

An intelligent energy management system using mixed-integer linear programming EMS-MILP for smart form sustainable power generation and delivery optimization for an H-MG structure is demonstrated. The stochastic optimization algorithm devised for H-MG outperforms its conventional counterpart under different load patterns, wide ranges of non-dispatchable/dispatchable DER installation capacity and electricity economization. In specific, using fast computational timesteps of about ~ 30 s, accuracy to produce higher accuracy, compatibility, extendibility and flexibility, for both offline and online power and energy distribution in H-MG applications. The optimization reduces energy costs due to non-dispatchable DER installation, and decreases the systems' dependence on traditional centralized generations. Also, where a combination of proposed ES and RLD integrated structure help not only to reduce the operational cost of the H-MG, but also to prevent unwanted events to effect system performance. The above concept signifies how an increase in the number of H-MGs in a multiple electrically/thermal coupled global grid system reduces the operational cost and/or maximizing profit at initial stages before dynamic variability's, cost starts to increase. In addition, the optimization highlights full control agility of generation and consumption trends to maintain maximize/minimize its economical profit/operational cost by making an intelligent power balance and exchange for H-MGs with upstream global grids at all times. Numerical simulations show the effectiveness of EMS-MILP algorithm in optimizing a moderate correlation between ES and RLD integrated H-MGs. In specific, this is advantageous to, stationary ES to store excess power generated in economically expensive Microgrids, where effective and cost reduction functionality can be achieved by this optimization strategy by integrating a RLD schedule in real-time. The stochastic optimization algorithm also offers ability for power system administrators to further enhance operational efficiencies for grid-connected integrated H-MG structures with different non-dispatchable /dispatchable DER resources. In summary, the proposed methodology can be fully incorporated for all global H-MGs with integrated multivariate renewable energy generation, distribution resources and loads under optimal real-time better management, performance and scheduling, adaptable versatile industrial standards and compliances.

7. Acknowledgments

This research is funded by the European Commission under contract "FP7-2013-NMP-ENV-EeB" through the Design4Energy project (Grant agreement no: 609380).

References

References

- [1] K. Chandrasekaran, S. P. Simon, Development of sustainable energy on generation system leads to eco-friendly society, *Sustainable Cities and Society*, 8 (2013) 1–15.

- [2] A. Ogunjuyigbe, C. Monyei, T. Ayodele, Price based demand side management: A persuasive smart energy management system for low/medium income earners, *Sustainable Cities and Society*, 17 (2015) 80–94.
- [3] M. Marzband, F. Azarnejadian, M. Savaghebi, J. M. Guerrero, An optimal energy management system for islanded microgrids based on multiperiod artificial bee colony combined with markov chain, *IEEE systems journal*, PP (99) (2015) 1–11.
- [4] M. Marzband, M. Ghadimi, A. Sumper, J. L. Domínguez-García, Experimental validation of a real-time energy management system using multi-period gravitational search algorithm for microgrids in islanded mode, *Applied Energy*, 128 (0) (2014) 164–74.
- [5] M. Marzband, N. Parhizi, J. Adabi, Optimal energy management for stand-alone microgrids based on multi-period imperialist competition algorithm considering uncertainties: experimental validation, *International Transactions on Electrical Energy Systems*, 30 (1) (2015) 122–31.
- [6] D. Parra, G. S. Walker, M. Gillott, Modeling of PV generation, battery and hydrogen storage to investigate the benefits of energy storage for single dwelling, *Sustainable Cities and Society*, 10 (2014) 1–10.
- [7] R. Lamedica, S. Teodori, G. Carbone, E. Santini, An energy management software for smart buildings with V2G and BESS, *Sustainable Cities and Society*, 19 (2015) 173–83.
- [8] L. Montuori, M. Alcázar-Ortega, C. Álvarez-Bel, A. Domijan, Integration of renewable energy in microgrids coordinated with demand response resources: Economic evaluation of a biomass gasification plant by homer simulator, *Applied Energy*, 132 (2014) 15–22.
- [9] A. A. Hamad, E. F. El-Saadany, Multi-agent supervisory control for optimal economic dispatch in DC microgrids, *Sustainable Cities and Society*, (2016) 1–9.
- [10] M. Mazidi, A. Zakariazadeh, S. Jadid, P. Siano, Integrated scheduling of renewable generation and demand response programs in a microgrid, *Energy Conversion and Management*, 86 (2014) 1118–27.
- [11] V. Mohan, J. G. Singh, W. Ongsakul, M. R. Suresh, Performance enhancement of online energy scheduling in a radial utility distribution microgrid, *International Journal of Electrical Power & Energy Systems*, 79 (2016) 98–107.
- [12] M. Marzband, N. Parhizi, M. Savaghebi, J. Guerrero, Distributed smart decision-making for a multimicrogrid system based on a hierarchical interactive architecture, *IEEE Transactions on Energy Conversion*, 31 (2) (2016) 637–48.
- [13] M. Marzband, A. Sumper, M. Chindriş, B. Tomoiagă, Energy management system of hybrid microgrid with energy storage, *The International Word Energy System Conference (WESC)*, Suceava, Romania, 2012.
- [14] M. Marzband, A. Sumper, J. L. Domínguez-García, R. Gumara-Ferret, Experimental validation of a real time energy management system for microgrids in islanded mode using a local day-ahead electricity market and MINLP, *Energy Conversion and Management* 76 (0) (2013) 314–22.
- [15] M. Marzband, A. Sumper, A. Ruiz-Álvarez, J. L. Domínguez-García, B. Tomoiagă, Experimental evaluation of a real time energy management system for stand-alone microgrids in day-ahead markets, *Applied Energy* 106 (0) (2013) 365–76.
- [16] M. Marzband, M. M. Moghaddam, M. F. Akorede, G. Khomeyrani, Adaptive load shedding scheme for frequency stability enhancement in microgrids, *Electric Power Systems Research*, (2016) 1–11.
- [17] M. Marzband, A. Sumper, O. Gomis-Bellmunt, P. Pezzini, M. Chindriş, Frequency control of isolated wind and diesel hybrid microgrid power system by using fuzzy logic controllers and PID controllers, in: *Electrical Power Quality and Utilisation (EPQU)*, 2011 11th International Conference on, 2011, pp. 1–6.
- [18] M. Marzband, Experimental validation of optimal real-time energy management system for microgrids, Phd thesis, Departament d'Enginyeria Elèctrica, EU d'Enginyeria Tècnica Industrial de Barcelona, Universitat Politècnica de Catalunya (2013).
- [19] M. Marzband, E. Yousefnejad, A. Sumper, J. L. Domínguez-García, Real time experimental implementation of optimum energy management system in stand-alone microgrid by using multi-layer ant colony optimization, *International Journal of Electrical Power & Energy Systems* 75 (2016) 265–74.

- 1 [20] M. Moafi, M. Marzband, M. Savaghebi, J. M. Guerrero, Energy man-
2 agement system based on fuzzy fractional order PID controller for tran-
3 sient stability improvement in microgrids with energy storage, *Inter-
4 national Transactions on Electrical Energy Systems* (2016) 1–20.
- 5 [21] A. Chabaud, J. Eynard, S. Grieu, A new approach to energy resources
6 management in a grid-connected building equipped with energy pro-
7 duction and storage systems: A case study in the south of france, *En-
8 ergy and Buildings*, 99 (2015) 9–31.
- 9 [22] M. Marzband, M. Javadi, J. L. Domínguez-García, M. M. Moghaddam,
10 Non-cooperative game theory based energy management systems for
11 energy district in the retail market considering DER uncertainties, *IET
12 Generation, Transmission & Distribution*, 10 (2016) 2999–3009.
- 13
14
15
16
17
18
19
20
21
22
23
24
25
26
27
28
29
30
31
32
33
34
35
36
37
38
39
40
41
42
43
44
45
46
47
48
49
50
51
52
53
54
55
56
57
58
59
60
61
62
63
64
65